

## COMPARATIVE SEISMIC PERFORMANCE OF REINFORCED CONCRETE VERSUS REINFORCED MASONRY STRUCTURAL WALLS

O. El-Azizy<sup>1</sup>, W.W. El-Dakhkhni<sup>2</sup> and Robert Drysdale<sup>3</sup>

<sup>1</sup> PhD student, Department of Civil Engineering, McMaster Univ., Hamilton, Canada. elazizo@mcmaster.ca

<sup>2</sup> PhD, Martini, Mascarin and George Chair in Masonry Design, McMaster Univ., Canada. eldak@mcmaster.ca

<sup>3</sup> PhD, Professor Emeritus, McMaster Univ., Hamilton, Canada. drysdale@mcmaster.ca

### ABSTRACT

Two Reinforced Concrete structural walls were compared to two Reinforced Masonry (RM) structural walls. The RM walls configurations were rectangular and boundary elements previously reported [1]. The reinforced concrete (RC) walls were constructed with the exact outer dimensions with the two different configurations. The RC had the same axial load applied and similar theoretical and experimental curvature ductility  $\mu_\phi$ . All the walls were three-story half-scaled. The RC walls were designed according to the Canadian concrete design code, CSA A23.3-04[2]. Lateral actuator was used to simulate the seismic loading connected to the top of the wall. Applying a fully cyclic lateral loading on the walls was the loading procedure in this experimental research. Potentiometers were placed at various locations to calculate lateral displacements, sliding and to compute the average curvature profile. All the walls failed in a flexural manner. The hysteresis loops, curvature profiles and the failure mode for each wall were discussed. Rectangular RC and RM walls had the same ultimate top drift of 1.2 % while the boundary elements RC and RM walls exerted ultimate top drifts of 1.58% and 2.40%, respectively. The load envelope of all the walls were plotted and compared. RM exerted higher displacement ductility  $\mu_\Delta$  compared to its RC counterparts. The RM walls had  $\mu_\Delta$  of 5 and 10 for the rectangular and the boundary element wall, compared to 4 and 6 for their corresponding RC walls.

**KEYWORDS:** boundary elements, curvature ductility, curvature profile, hysteresis loops, reinforced concrete, reinforced masonry

### BACKGROUND

The highest values of the ductility related- seismic force response modification factor ( $R_d$ ) in the National Building Code of Canada are 2.0 and 3.5 for reinforced masonry (RM) and reinforced concrete (RC) cantilever shear walls, respectively[3]. The  $R_d$  values for RM shear wall Seismic Force Resisting System (SFRS) in the NBCC are especially conservative compared to other similar SFRS. The objective of the research is to conduct an experimental study focusing on directly comparing the differences between RC and RM structural walls that might create a case for change in future editions of the NBCC. Moreover, the experimental results will contribute to the masonry seismic performance database that is essential to facilitate the shift from the force-based design approach to performance-based design methodologies [4]. Possible shift to performance-based design methodologies will be considered as of the NBCC 2020 edition,

as a part of the efforts of the Canadian Standing Committee on Earthquake Design (SC-ED). Detailing and confinement plays a major role in enhancing the seismic performance of both RM and RC structural wall. Having two layers of vertical reinforcement, within confined boundary elements, also limit out-of-plane displacement and enhance wall stability under inelastic strains [5].

## Experimental Work

### Material and properties

Two RC structural walls were tested under fully-reversed cyclic loading in the Applied Dynamics Laboratory (ADL) of McMaster University. The test results were discussed and compared to two RM structural walls counterparts that were already tested and reported earlier by (Shedid et al., 2010) [1].

#### *RC Walls*

Three different reinforcement sizes were used for the half-scale walls, namely: D4, D7 and D11 bars that correspond to M10 ( $A=100 \text{ mm}^2$ ), M15 ( $A=200 \text{ mm}^2$ ) and M20 ( $A=300 \text{ mm}^2$ ) in full-scale. The D4, D7 and D11 bars have cross sectional areas of 26, 45 and 71  $\text{mm}^2$ , respectively. The D4 bars were used as the confinement in the boundary most critical region and horizontal reinforcements. The D11 bars were used as the vertical reinforcement of the rectangular wall and the confined regions of the boundary element wall. While, the D7 bars were used as the distributed vertical reinforcements for the boundary element wall. Tensile testing were performed on D4, D7 and D11 bars exerting average yield strength of 510 MPa, 480 MPa, 420 MPa, respectively. The D4, D7 and D11 had average Young's moduli of 206 GPa, 198 GPa and 201 GPa, respectively.

The two walls were poured with the same mix with a maximum aggregate size of 10 mm, which corresponds to a full-scale wall with 20 mm maximum aggregate size. Eighteen cylinders were prepared and tested under compression; three cylinders were tested after 7 days of the pour, three after 14 days, three after 28 days and three cylinders were tested after 60 days. Moreover, three cylinders were tested on each wall-testing day. The slump was 210 mm. The average concrete compressive strength for the RC walls was 42 MPa [6].

#### *RM Walls*

Available M10 bars were used as the vertical reinforcements of the RM walls. The bars had an average yield strength of 495 MPa and the average Young's Modulus was 200.6 GPa. The wall horizontal reinforcement consisted of D4 bars and had average yield strength of 534 MPa.

Half-scaled block, representing the standard hollow 20-cm block, were tested under compression in accordance with CSA A165 [7]. The blocks average compressive strength was 27.2 MPa. The grout used to fill the walls exerted an average compressive strength of 21.8 MPa. Three fully grouted four-block high prisms were constructed and grouted at each construction stage. The prisms were tested and exerted average compressive strength of 16.4 MPa. According to the ASTM C1314-06 [8], two-block high prism with height to thickness ratio of 2 is considered to represent masonry compressive strength. As such, when multiplying the compressive strength by a 1.15 modification factor, the ASTM-based masonry compressive strength becomes 18.8 MPa.

### Wall Design and Construction

The experimental comparative research included four walls; two rectangular (RC and RM) and two end-confined (RC and RM). All the three-story walls had the same height and length (3,990 mm × 1,802 mm) that resulted in an aspect ratio of 2.2. The storey height was 1,230 mm in addition to 100 mm thick slab that extended 150 mm from both sides as shown in Figure 1(c).

#### RC Walls

The rectangular and end-confined RC walls were designed as ductile structural walls according to the CSA A23.3-04 [2]. The forms were built side ways and the steel reinforcement cages were tied and placed in the forms as shown in Figure 1(a). Following that, premixed concrete was used to fill the wall, foundation and slabs. The rectangular wall vertical  $\rho_v$  and horizontal  $\rho_h$  reinforcement ratios were 2.80 % and 1.1 % respectively. While the end-confined  $\rho_v$  and  $\rho_h$  reinforcement ratios were 1.63 % and 1.05 % respectively.

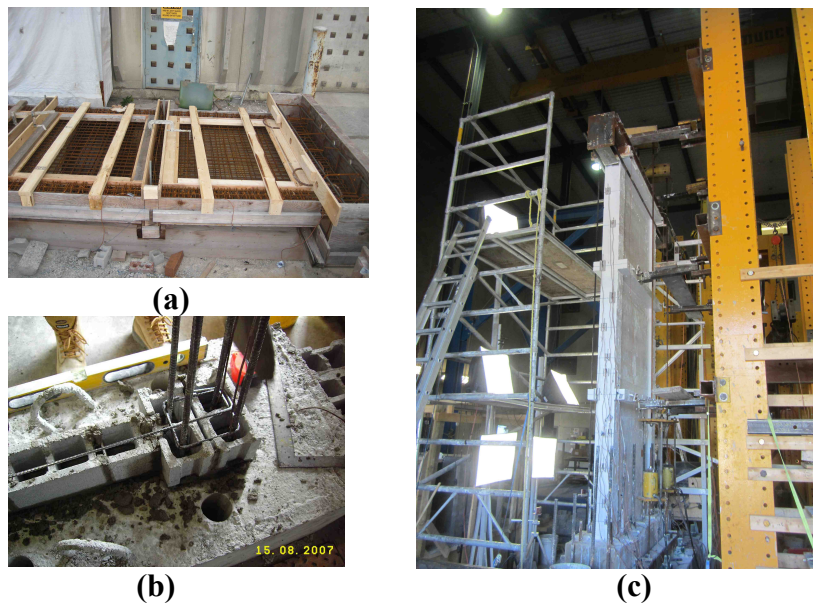


**Figure 1: (a) RC steel cages in the forms, (b) First course construction of the RM end-confined walls. (c) RC End-confined wall test setup**

#### RM Walls

The rectangular and end-confined RM walls were designed as moderately ductile walls according the CSA S304-04 [9]. An experienced mason built each wall in six stages. Each stage comprised half a story height. The horizontal reinforcement was placed in the courses during construction in pre-notched block as shown in Figure 1(b). Grouting was performed the next day after the construction of each half a story. When grouting of each full story was completed, wooden forms were constructed for the storey and roof slabs. One day after the concrete was poured in the slab, the mason continued building the second story. The same procedure was repeated until the concrete roof slab was poured. The end-confined areas were constructed by laying two concrete blocks at each end as shown in Figure 1(b). The vertical reinforcement ratios

for the RM walls  $\rho_v$  were 1.17 % and 0.55 % for the rectangular and end-confined walls, respectively. While the horizontal reinforcement ratio  $\rho_h$  was 0.3 % for both walls [1].

### Test Matrix

The two RC walls were specifically designed to be directly comparable to their RM counterpart as all walls were designed to have similar theoretical and experimental curvature ductility  $\mu_\phi$  values as summarized in Table 1. The theoretical and experimental yield and ultimate curvature of RM walls and RC walls are also included in Table 1. For the RC Structural walls, the experimental curvature ductility  $\mu_\phi$  of the rectangular wall was almost identical to the theoretical  $\mu_\phi$ . Moreover, the rectangular RC wall (RCR) yield curvature  $\phi_y$  and ultimate curvature  $\phi_u$  theoretical versus experimental values are very similar. However, the experimental curvature ductility  $\mu_\phi$  for the end-confined RC wall (RCE) was lower than the predicted value as the experimental ultimate curvature  $\phi_u$  was lower than the corresponding theoretical value. The RCE wall experimental yield curvature  $\phi_y$  was similar to the theoretical yield curvature  $\phi_y$ . The experimental yield curvatures  $\phi_y$  of the RM walls were similar to the corresponding theoretical values. In the rectangular RM wall (RMR) the experimental ultimate curvature  $\phi_u$  and curvature ductility  $\mu_\phi$  were slightly higher than the theoretical values. Finally, the end-confined RM wall (RME) exerted slightly lower experimental ultimate curvature  $\phi_u$  and curvature ductility  $\mu_\phi$  values compared to the predicted values.

**Table 1: Theoretical and Measured wall curvatures  $\phi$  and curvature ductility levels,  $\mu_\phi$ , of the RC structural walls Versus the RM structural walls**

	Reinforced Concrete Structural Walls				Reinforced Masonry Structural walls			
	Rectangular RCR		End-confined RCE		Rectangular RMR		End-confined RME	
	Theo.	Exp.	Theo.	Exp.	Theo.	Exp.	Theo.	Exp.
Yield curvature $\phi_y \times 10^{-6}$ (rad/mm)	1.76	1.41	1.59	1.43	1.92	1.88	1.85	1.91
Ultimate curvature $\phi_u \times 10^{-6}$ (rad/mm)	7.78	6.89	17.09	11.65	5.61	7.77	14.36	12.49
Curvature ductility $\mu_\phi$	4.42	4.89	10.75	8.15	3.00	4.13	7.80	6.54

### Test Setup

The axial loads on the wall were applied through two hydraulic actuators and threaded rod system connected to two steel box sections on the top of the walls. The axial load added is equivalent to the load of the tributary area the wall is supposed to support. The four walls had the same axial load of 160 kN (corresponding to the same tributary area). Figure 2(b) shows the layout of the axial load application system. A quasi-static fully reversed lateral loads were applied on the top of the wall. The top wall actuator was connected to the wall via a U-shaped built up steel-loading beam as shown in Figure 2(a). The steel-loading beam was welded to the vertical reinforcements after laying it down on a layer of mortar for leveling which creates a zero moment on the top of the wall. The loading commences by applying two full push and pull cycles then back to zero load on each stage. The walls were loaded at 20, 40, 60 and 80% of the theoretical yield strength. The fifth loading stage the wall was loaded until each wall developed

its experimental yield strength. The experimental yield strength and displacement were identified via the electric strain gauges connected to the outer most steel reinforcement at the interface. After reaching the yield strength  $F_y$  and the corresponding yield displacement  $\Delta_y$ , the loading protocol switched to displacement-controlled loading targeting integer multiples of  $\Delta_y$  until the wall strength degrades to 50% of the ultimate strength, at which point the test will be terminated [6].

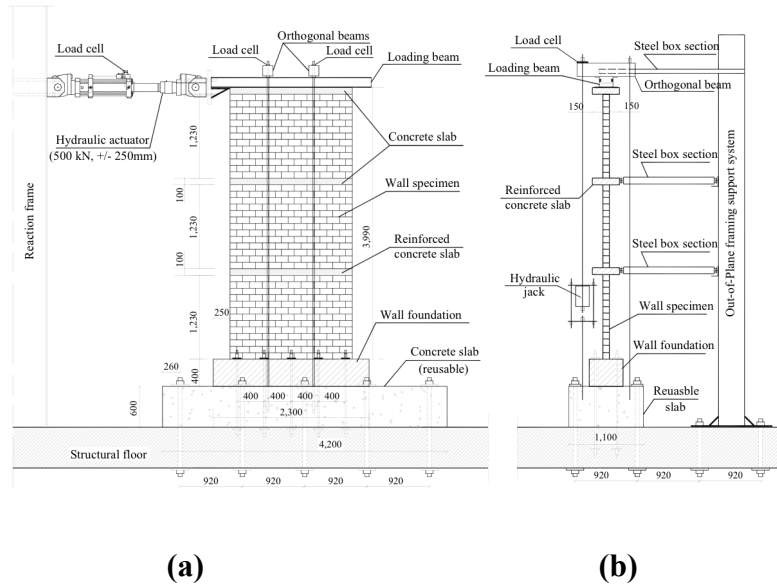


Fig. 2: (a) Test Setup (b) Axial load and out of plane supports [6]

## Instrumentations

### RC Walls

Nine displacement potentiometers were placed to measure the lateral displacements along the height of the wall. In addition, thirteen displacement potentiometers were mounted on each side of the wall to calculate the curvature as shown in Figure 1(c). A displacement potentiometer was mounted at the wall-base interface to measure any possible sliding. Seven strain gauges were attached to two of the outer most vertical bars. One bar had five strain gauges located at 200 mm below the interface, at the interface, 100 mm above the interface, at a height equal to half the wall length 901 mm ( $l_w/2$ ) and at a height equal to the wall length ( $l_w$ ) 1,802 mm from the wall-base interface. The second bar had two strain gauges located at 50 mm above the interface and at a height of 1,802 mm from the interface (the full wall length  $l_w$ ).

### RM walls

Seven displacement potentiometers were located along the height of the wall to measure lateral displacements. Eleven displacement potentiometers were mounted along the height of the wall on each side to calculate the wall curvature. One displacement potentiometer was placed at the wall-base interface to measure any possible sliding. Four strain gauges were attached to the outer most vertical reinforcement on each side to measure the yield displacement and the extent of

plasticity. The strain gauges were located on each side of the wall at 200 mm below the interface, at the interface, 400 mm above the interface and 800 mm above the interface.

### Test Results

The comparative study reported in this paper focuses on comparing the load-displacement relationships and the failure modes of the RM walls and their RC wall counterparts. In addition, further analysis compares the walls curvature profiles, curvature ductility level,  $\mu_\phi$  and displacement ductility level,  $\mu_\Delta$ .

### Load-displacement Relationships

The load displacement relationships were generated as shown in Figure 3. The first quadrant shows the hysteresis loops in the push direction while the third quadrant shows it in the pull direction. The top left table indicates the yield loads, ultimate capacities and the 80% strength degradation loads and displacements. The ultimate displacement of the wall was the displacement at 80% of the ultimate strength degradation. The bottom right table summarized the wall key features including: the wall length,  $L_w$ , and height,  $h_w$ , the vertical,  $\rho_v$ , and horizontal,  $\rho_h$ , reinforcement ratios and the axial load,  $P$ , applied on the wall.

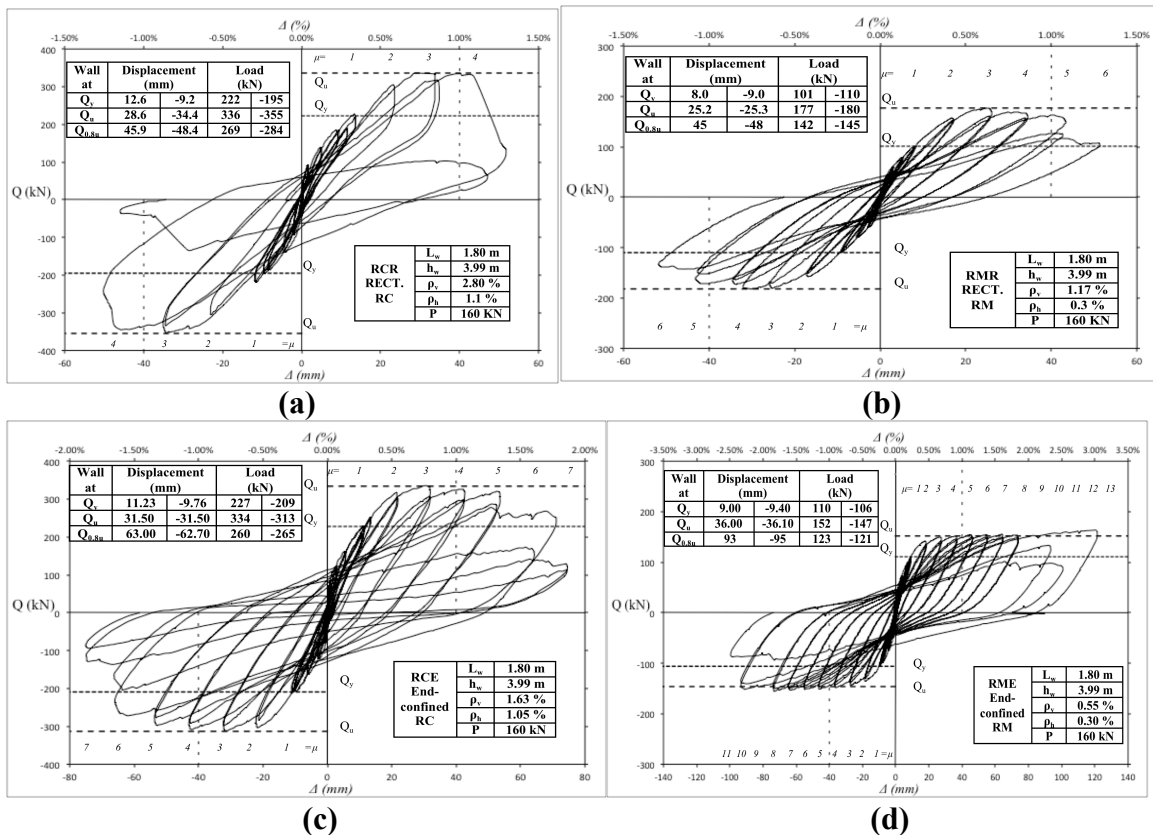


Figure 3: Hysteresis loops of (a) RC Rectangular wall RCR (b) RM Rectangular wall RMR (c) RC End-confined wall RCE (d) RM End-confined wall RME

## Failure Modes

### *RCR Walls*

The wall failed in a flexural manner as the concrete crushed at the compressive toes at both sides and the bars started to buckle at the first push and pull cycles of  $4\Delta_y$ . The two outer most steel bars fractured on each side at the second push and pull cycle of  $4\Delta_y$  load. As a result, the wall strength degraded very rapidly after the  $4\Delta_y$  cycle and an offset occurred as shown in Figure 4(a) and the test was terminated. The wall first flexural crack occurred at 60% of the theoretical yield,  $F_y$  (at a load of 140 kN) and was located in the bottom third of the first story. At 80%  $F_y$ , more flexural cracks start to develop at the first floor and two cracks at the bottom of the second story. At  $F_y$ , diagonal shear cracks and further flexural cracks developed within the first story and the bottom half of the second story. However, minimal flexural cracks were observed at the third story and the top half of the second story. At the  $2\Delta_y$  and  $3\Delta_y$  displacement cycles, extensive diagonal shear cracking occurred at the first story, moderate amount in the second story and very minimal diagonal shear cracks in the third story. The ultimate failure occurred at  $4\Delta_y$  cycles where, as shown in Figure 3(a), extensive concrete crushing at the wall toe was apparent.

The wall yielded at a top drift of 0.33 % and 0.24 % in the push and pull directions, respectively. The yield loads were 227 kN and 195 kN in the push and pull directions, respectively. After reaching a load corresponding to  $\Delta_y$ , the wall continued to carry more load with more energy dissipation shown in Figure 3(a) as the loops became fatter. At the  $3\Delta_y$  load the wall reached its ultimate strength of 336 kN and 355 kN in the push and pull direction, respectively, corresponding to 0.85% top drift. After  $3\Delta_y$ , the wall strength slightly degraded up to the  $4\Delta_y$  (1.13 % top drift) displacement. The ultimate displacement of the wall was 1.15% and 1.21% for the push and pull direction, respectively. At the second  $4\Delta_y$  cycle the wall strength was not gained as required and the test was terminated.

### *RMR Walls*

As expected, the wall failed in flexure with most of the cracks occurring in the first story. The second story had significantly less cracks and very minimal cracks occurred in the third story. At the  $\Delta_y$  cycle, horizontal flexural cracks were visible all over the first story and the bottom two courses of the second story. Vertical cracks followed by toe crushing in both ends, accompanied by diagonal shear cracks in the first story occurred at  $3\Delta_y$ . At  $4\Delta_y$ , masonry face shell spalling started to occur with the face shell splitting at both wall toes at  $5\Delta_y$ . In addition, one of the end steel bar buckled as shown in Figure 4(b). At  $6\Delta_y$ , the same steel bar fractured and the wall strength degraded to 50% of its ultimate, and subsequently the test was terminated.

The wall yielded at 0.21 % top drift with a load of 101 kN in the push and -110 kN in the pull. The ultimate loads were of 177 kN and 180 kN in the push and pull respectively with a corresponding top drift of 0.62%. The ultimate top displacement recorded was 1.17 %.

### *RCE Walls*

The first crack in this wall occurred at 60%  $F_y$  at the bottom third of the first story. At 80%  $F_y$  flexural and shear diagonal cracks occurred at the first story. While at  $F_y$  load diagonal cracks were visible in the second story coupled with an increase of the shear diagonal cracking in the first story. The diagonal shear cracks increase significantly in the first and second story at  $2\Delta_y$  and  $3\Delta_y$  displacement cycles. At  $3\Delta_y$  load vertical cracks around the toes were visible. At  $4\Delta_y$ ,

uplifting in the tension side starts occurring and minor concrete spalling was visible in the compression zone. At  $5\Delta_y$ , toe crushing occurred at both sides seven reinforcement bars buckled in the east boundary element while four bars buckled in the west boundary element. At  $6\Delta_y$ , four vertical reinforcement bars fracture in at one end and two other in the other end. In the East direction four more bars snapped at  $7\Delta_y$  load, two bars were in the confined region and the other two were in the distributed wall web mesh. In the West toe seven vertical reinforcement bars located in the boundary element region snapped. At  $8\Delta_y$ , all the vertical reinforcement bars in the confined regions fractured as shown in Figure 4(c) in addition to the outer four vertical bars in the East side and two in the West sides of the wall web. The wall experienced at almost the same load and displacement as the RCR. The hysteresis loops continued to widen and energy dissipation increased after yielding. The ultimate load drift was 0.79%, occurring at  $3\Delta_y$  cycle, with a push load of 334 kN and a pull load of 313 kN. The ultimate displacement of the wall was 1.58%. At the  $8\Delta_y$  cycle the wall strength degraded to 50% of the ultimate strength and the test was terminated.

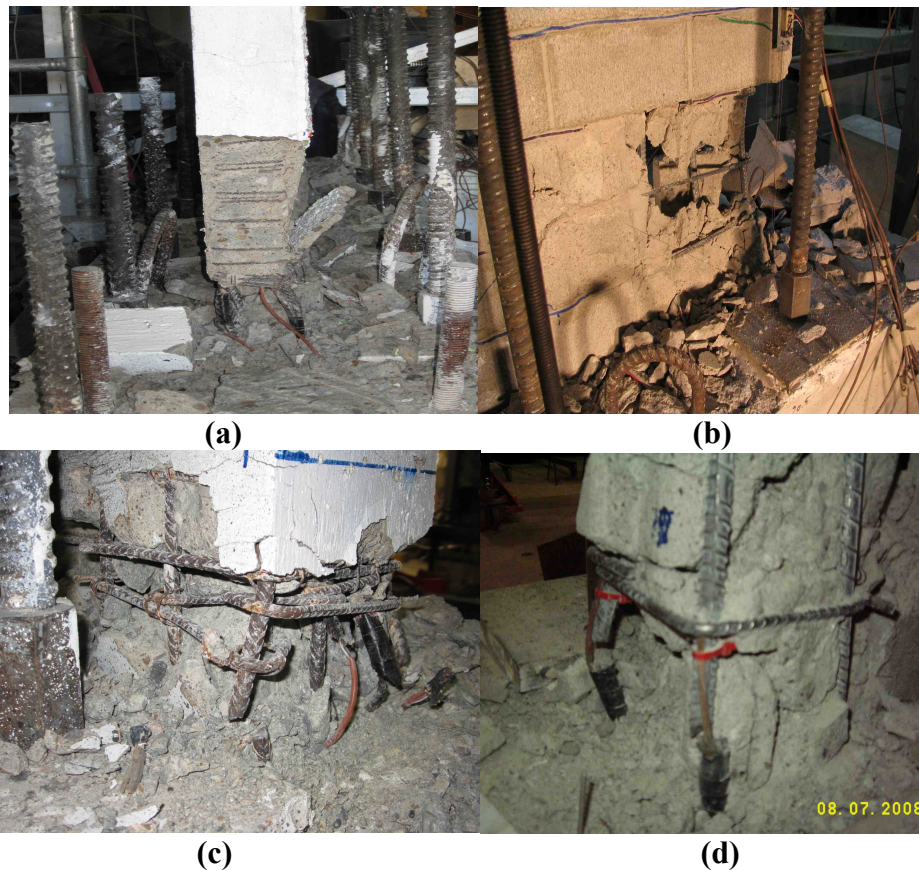


**Figure 4: Toe crushing and bar snapping (a) RCR (b) RMR (c) RCE (d) RME**

*RME Walls*

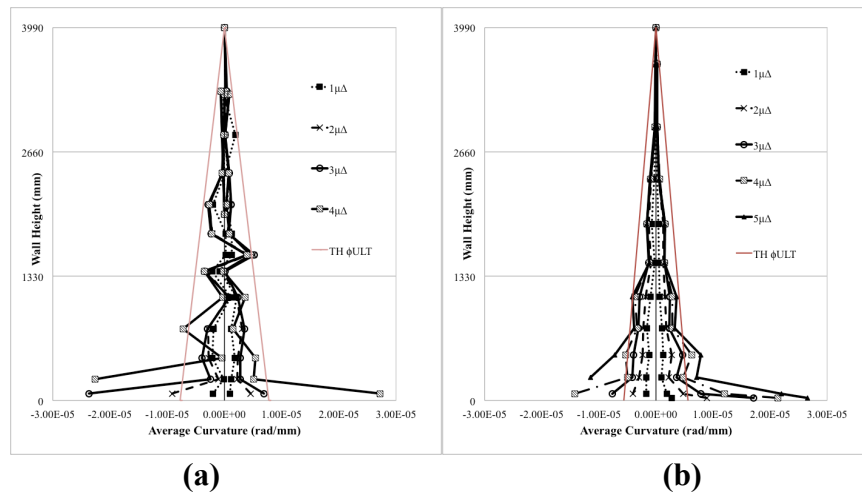
The wall failed in a flexural manner with a similar crack pattern to the RMR wall. Flexural cracks propagated from the interface up to the second bed joint in the second story at  $\Delta_y$  level. At  $3\Delta_y$ , diagonal shear cracks were seen in the first story. At  $6\Delta_y$ , vertical and horizontal cracks were



observed at both toes while, at  $7\Delta_y$ , the vertical cracks propagated to the second course and major cracks occurred at the flange. At the first cycle of  $8\Delta_y$ , face shell separation at the boundary element and at the end zone of the web occurred. Grout also started to spall within the bottom two courses in the second cycle of  $8\Delta_y$ . Due to a problem in the top potentiometer, the wall was pushed to a displacement corresponding to  $13.5\Delta_y$  instead of  $9\Delta_y$  that resulted in reinforcement bars buckling following crushing of the surrounding grout. Following that, it was decided to load to  $10\Delta_y$  in the push direction, which resulted in a similar damage to that in the pull direction. At  $11\Delta_y$ , the outer most two vertical bars fractured, the wall strength degraded to 50% and the test was terminated. The wall yielded at 0.23% top drift exerting a push loads of 110 kN and 106 kN, respectively. After yield the hysteresis loops widens which show the energy dissipation and the wall ductile capability. The ultimate strengths of the wall were 152 kN and 147 kN in the push and pull directions, respectively, corresponding to a 0.9% top drift. The wall exerted an ultimate top drift of 2.4%.

### Curvature profiles

The average curvature profiles were calculated based on strain measurements. Average curvatures along the height were plotted for each wall as shown in Figure 5. Theoretical ultimate curvatures  $\phi_{uTh}$  were plotted on each curvature profile to compare the experimental ultimate curvature versus the predicted curvatures. The experimental average ultimate curvatures at the bottom 150 mm were very similar for both of the rectangular walls with ultimate curvatures  $\phi_u$  of  $6.89 \times 10^{-6}$  and  $7.77 \times 10^{-6}$  (rad/mm), for the RCR and RMR walls, respectively. The same values were  $11.65 \times 10^{-6}$  and  $12.49 \times 10^{-6}$  (rad/mm) for the RCE and RME walls, respectively.



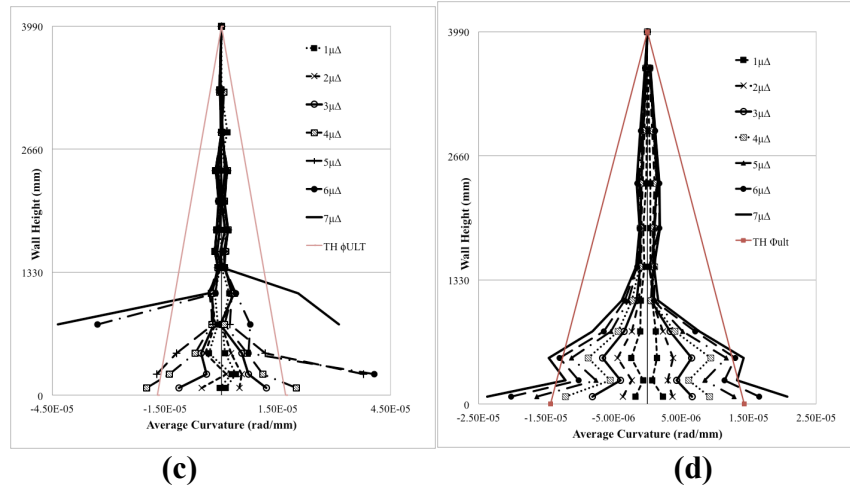


Figure 5: Curvature Profile over the height (a) RCR (b) RMR (c) RCE (d) RME

**Displacement ductility  $\mu_{\Delta}$  and Curvature ductility  $\mu_{\phi}$**

The rectangular and end-confined RC and RM walls load-displacement relationships are shown in Figure 6. The wall strengths were normalized to account for the difference in the wall capacities between RC and RM. All walls failed in a ductile manner and showed high ductile capabilities. The rectangular walls reached almost the same ultimate displacement. After yield, the RMR wall reached higher load levels at a lower top percentage drift than the RCR up to 0.75% and 0.80 % top drift in the push and pull direction, respectively. After that, the RCR gained strength while the RMR wall strength was degrading. The RCR wall strength degradation occurred in a less ductile manner compared to the RMR wall. Regarding the end-confined walls, both walls had the same yield displacement in the pull direction, but the RCE wall had a higher yield displacement in the push direction. The RME wall had higher ultimate displacement than RCE. Both the RME and RCE walls gained strength at almost the same rate after yield. The RCE wall strength degradation was more brittle than RME strength degradation as shown in Figure 6(b).

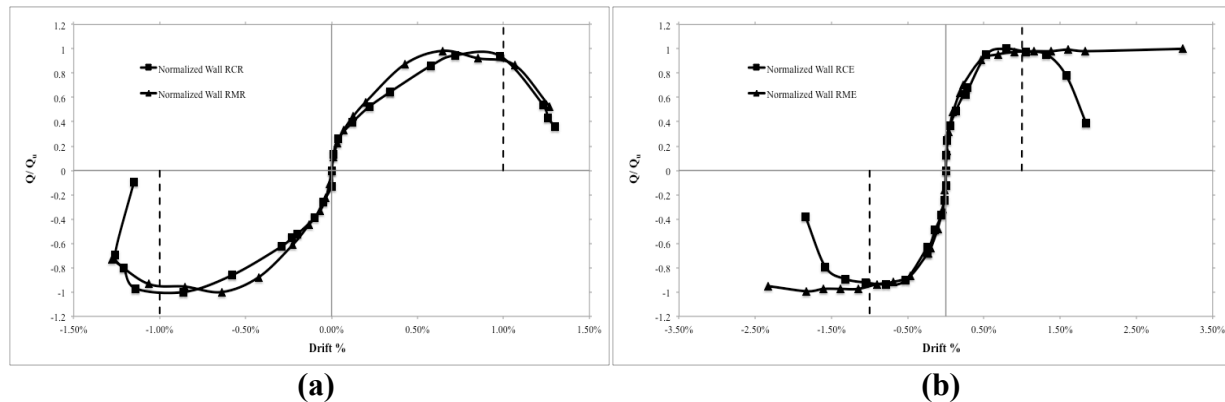


Figure 6: Load-displacement envelopes (a) The Rectangular walls (b) The End-Confined walls

The rectangular walls had very similar curvature ductility levels,  $\mu_\phi$ , as the RCR was 4.42 while RMR was 4.13. The RMR exerted a higher displacement ductility  $\mu_\Delta$  of 5.0 compared to RCR of 4.0  $\mu_\Delta$ . The curvature ductility  $\mu_\phi$  in the RCE was 8.15, which is higher than RME ( $\mu_\phi=6.54$ ) by 20%. While, the RME wall exerted higher displacement ductility  $\mu_\Delta$  of 10.0 compared to 6.0 that was experienced by the RCE wall. This indicates that, despite the fact that the RC wall had higher curvature ductility levels, the RM walls developed higher displacement ductility levels compared to their RC counterparts. This might be attributed to the fact that the RC wall inelastic curvature profile covered a shorter distance (plastic hinge length) along the wall height compared to their RM counterparts. The experimental results are currently being further investigated to develop an analytical model to evaluate the effect of different parameters on all the tested wall ductility and top wall drift levels.

### Conclusions

In this experimental research, Reinforced Masonry walls showed a much better seismic performance compared to their Reinforced Concrete counterparts. Moreover, The boundary elements walls showed tremendous ductile capability compared to the rectangular walls. Boundary elements RM and RC walls have higher displacement ductilities  $\mu_\Delta$  by 50 % and 33 % compared to their rectangular counterparts. RM structural walls ductility related response modification factor  $R_d$  is extremely conservative in the NBCC. The experimental research verified that Reinforced Masonry walls having the same curvature ductilities  $\mu_\phi$  of Reinforced Concrete structural walls could seismically perform better. As the experimental displacement ductilities  $\mu_\Delta$  in the RM walls are 20% and 40 % higher in the rectangular and boundary elements walls respectively.

### Acknowledgements

Financial support has been provided by the McMaster Centre for Effective Design of Structures (CEDS) funded through the Ontario Research and Development Challenge Fund (ORDCF) as well as the Natural Sciences and Engineering Research Council (NSERC) of Canada. The continuous support of the McMaster Masonry Research Group (MMRG) by the Ontario Masonry Contractors Association (OMCA), the Canada Masonry Design Centre (CMDC) and the Canadian Concrete Masonry Producers Association (CCMPA) is gratefully acknowledged.

### References

- [1]Shedid, M., El-Dakhkhni, W., and Drysdale, R. (2010). "Alternative strategies to enhance the seismic performance of reinforced concrete-block shear wall system" J. Struct. Eng., 136(6), 676-689.
- [2] Canadian Standards Association (CSA). (2004-c). CSA A23.3-04 "Design of Concrete Structures" CSA A23.3-04, Mississauga, ON
- [3] NBCC 2010: National Research Council of Canada, "National Building Code of Canada", 2010.

- [4] Applied Technology Council. (ATC). (2006). “Next generation performance-based seismic design guidelines: Program plan for new and existing buildings.” Federal Emergency Management Agency (FEMA) 445, Washington D.C., USA.
- [5] Paulay, T., Priestley, M. (1992). “Seismic design of reinforced concrete and masonry buildings” Wiley, New York.
- [6] El-Azizy, O., El-Dakhakhni, W., Drysdale, R. (2012), “*Proposed Experimental Study to Compare the Seismic Performance of Reinforced Concrete and Reinforced Masonry Structural Walls*” 15<sup>th</sup> International Brick and Block Masonry Conference.
- [7] Canadian Standards Association (CSA). (2004-a). “Concrete Block Masonry Units” CSA A165, Mississauga, Ont., Canada
- [8] ASTM International. (2010). “Standard test method for compressive strength of masonry prisms.” C1314, West Conshohocken, Pa., (2010)
- [9] Canadian Standards Association (CSA). (2004-b). CSA S304.1-04 “Design of Masonry Structures” Canadian Standards Association (CSA). CSA, Mississauga, ON.